

Compact and Miniaturized Dual Band Tag Antenna Based on Metamaterial for IoT, RFID Technology, and Hospital Services Applications

Abdessalam El Yassini*, Mohammed Ali Jallal, Saida Ibnyaich, Abdelouhab Zeroual

Physics Department, Faculty of Sciences Semlalia, Cadi Ayyad University, 40000 Marrakesh, Morocco

(Received 05 October 2022; revised manuscript received 21 December 2022; published online 27 December 2022)

This research proposes a compact tag antenna for Radio Frequency Identification (RFID) which provides two bands of operation at 2.3-2.5 GHz and 5.78-6 GHz. The tag antenna structure consists of two meander lines connected with an inductive loop of the metamaterial. This design topology offers benefits such as achieving multi-band, good impedance matching and radiation pattern at resonant frequencies. The design has a small size of $16 \times 23 \times 1.6 \text{ mm}^3$. The suggested tag antenna is produced on top of the FR4 substrate having $\epsilon_r = 4.3$ and $\tan\delta = 0.022$. The tag antenna has a maximum gain of 2.14 dBi and 3.22 dBi at the resonant frequencies of 2.45 GHz and 5.8 GHz, respectively. The study of the suggested tag antenna with the human body, solution bag, and bandage is presented. In addition, the proposed tag antenna has good performance and supports two bands of operation, which confirms its suitability for RFID technology and remote healthcare applications.

Keywords: RFID tag, IoT, Metamaterial, Dual-band, Hospital services applications.

DOI: [10.21272/jnep.14\(6\).06013](https://doi.org/10.21272/jnep.14(6).06013)

PACS numbers: 84.40.Ba, 84.40.Lj

1. INTRODUCTION

Progressions on the internet of things (IoT) are more used for attaching several telecommunication systems like sensors, appliances, robotics, and other objects. All these devices may equip with radio frequency identification (RFID) tags, healthcare solutions, bio-industries sensors, and many other. The RFID technology is widely employed, due to its capacity to monitor the objects autonomously. In hospital departments, a healthcare system is generally used to facilitate the exchange of patient information [1].

Additionally, the control access to hospital services necessitates a solid security system, which may involve the usage of wristbands and RFID cards.

The reader, tag, and computer host are the main elements of the RFID system. Its mechanism of operation is dependent on a reader transmitting a modulated radio frequency signal to feed the passive tag. The tag is equipped with a microchip that is attached on an antenna. The reader has an ability to collect all data from the tag's chip. Host systems track and investigate information about an object [2]. Furthermore, the RFID data can be sent in a variety of frequency bands. The standard of 2.45 GHz and 5.8 GHz are mostly used in microwave frequencies [3].

In recent published studies, various antennas for RFID tag technologies have been presented; however, most of them have a single band of application, no compact size, and a short-read distance. RFID technology demands miniature antennas with better performances of gain, multi-band, and impedance matching. The tag antenna must be small and inexpensive in order to be associated with an object. Several approaches to improve the performance of antennas have been employed for example, the use the slots or parasitic components on the patch, and create a fractal design [4, 5].

The zeroth-order resonance (ZOR) approach offers the miniaturization, in this case the antenna generates

a resonant frequency that is independent to its surface area [6, 7]. Furthermore, the above approach provides a limited bandwidth. The alternative method relies on a series of closely spaced resonances with an appropriate frequency [8, 9]. The meander line improves the prolong of the surface current and allows designing a compact antenna.

The utilization of tag antennas in the area of healthcare has yielded greater benefits, such as making patients' lives easier, providing for greater surveillance and healthcare monitoring [10, 11]. In addition, RFID technology can be used in intelligent blood storage, locating a special blood pouch [12]. These applications necessitate the tagging of objects (such as the body, liquids, and plastics) that have an impact on the results of antenna in terms of radiation pattern and input impedance. A basic RFID system for healthcare applications is depicted in Fig. 1.

This work provides a detailed design methodology for developing a planar antenna attached to RFID wireless remote healthcare applications. A low profile, multi-standard tag is presented. The suggested structure comprises meander lines and a metamaterial structure providing two resonant frequencies. The rest of the work is composed of five sections. Section 2 presents the RFID tag. Section 3 presents the evolution of the tag antenna geometry. The results and discussion are presented in Section 4 and Section 5 draws some conclusions.

2. STRUCTURE AND DESIGN EVOLUTION OF THE TAG ANTENNA

2.1 Structure of the Tag Antenna

Fig. 2 shows the shape of the suggested tag antenna, it has a size of $16 \times 23 \times 1.6 \text{ mm}^3$. The RFID tag includes two principal parts, electronic chip and meander lines. The red part is meander lines, which has an

* abdessalam.elyassini@edu.uca.ac.ma

S-shaped structure. This tag is constructed from a FR4 epoxy substrate ($\epsilon_r = 4.3$) with a thickness of 1.6 mm. The tag is coupled to a reference ASIC [12] electronic chip. It has an input impedance $Z_{Ch1} = (28 - j111.9) \Omega$ and $Z_{Ch2} = (28 - j47.3) \Omega$ at a central frequency of 2.45 GHz and 5.8 GHz, respectively. T-matching is formed to modify the direction of the surface current. As a result, T-feed parameters are optimized to obtain the inductive and capacitive effect required for conjugate matching with the chip. The detailed parameters are shown in Table 1.

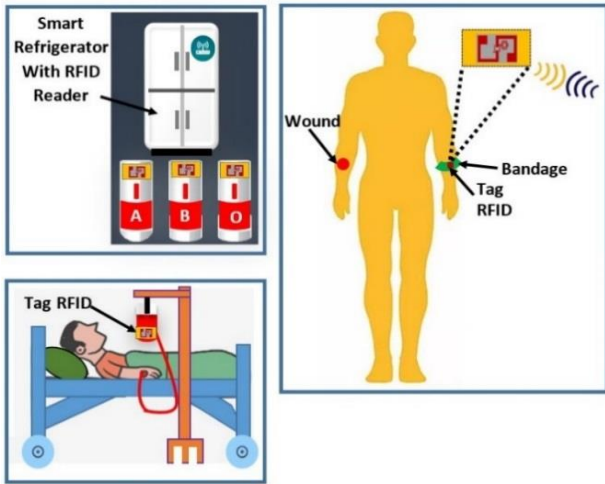


Fig. 1 – Schematic diagram of the designed tag antenna for healthcare applications

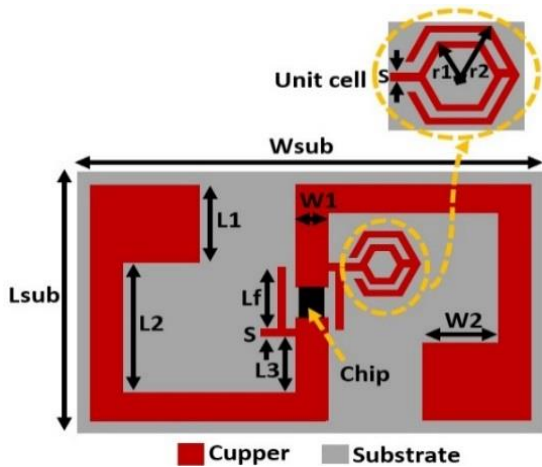


Fig. 2 – Tag antenna structure

2.2 Design Evolution of the Tag Antenna

The evolution of the recommended tag antenna has gone through three steps and various results of the reflection coefficient are presented in Fig. 3.

The first step presents conventional meander lines connected with a chip named Philips ASIC. It is observed that this structure provides a single bandwidth from 2.39 GHz to 2.50 GHz and a resonance frequency at 2.45 GHz with poor isolation below -10 dB ($S_{11} = -16.92$ dB) due to low impedance matching between the chip and the antenna. Therefore, the meander line is loaded with two T-shaped stubs (step 2) to achieve excellent impedance matching. This structure offers

better isolation at the operating frequency and the reflection coefficient is decreased to -30 dB. In the last design, the iterative structure is loaded with a resonating metamaterial ring. It is noticed that the second resonant frequency is created. The recommended antenna provides best reflection coefficients of -35 dB and -22 dB at frequencies of 2.45 GHz and 5.8 GHz, respectively.

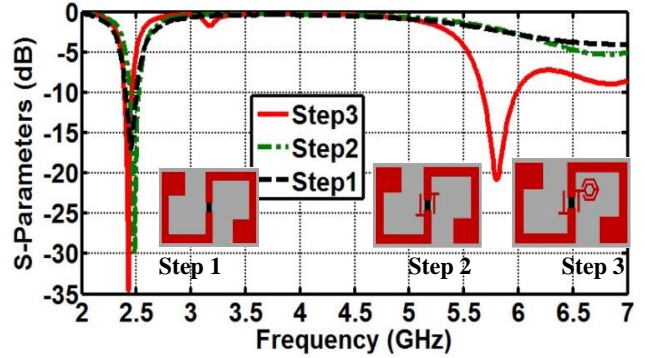


Fig. 3 – Reflection coefficient of the tag antenna

Table 1 – Dimensions of the suggested RFID tag

Parameters	Dimensions (mm)	Parameters	Dimensions (mm)
W_{sub}	23	r_2	2
r_1	2.4	W_2	3
L_{sub}	16	L_f	4.5
W_1	2	h	1.6
L_2	6	L_3	3.1
S	0.4	L_1	6

3. PARAMETRIC STUDY

The purpose of this section is to illustrate the effect of those parameters on the electrical performance of the tag antenna such as the impedance and the reflection coefficient S_{11} . The optimal values are given in Table 1. All simulations are achieved using CST MWS software.

3.1 Effect of the Length W_2 on the Tag Results

To notice the effect of varying length W_2 of the meander line on the operating frequency and the tag antenna impedance matching is increased from 2 to 5 mm.

Fig. 4 displays the results of the S-parameters with various values of W_2 . It is obvious from the obtained results that the first operating frequency is more affected by the parameter W_2 . In addition, it is noted that changing this length does not affect the second operating band. When $W_2 = 3$ mm, the tag antenna has two resonant frequencies around 2.45 GHz and 5.8 GHz, which correspond to the input impedances of $(28 + j130) \Omega$ and $(27 + j40) \Omega$, respectively, as indicated in Fig. 5.

3.2 Effect of the Length L_f on the Tag Results

The effect of modifying the length L_f on the antenna results in terms of reflection coefficient and input impedance has been studied. The L_f parameter varies from 4.5 to 7.5 mm in 1 mm increments. Fig. 6 shows

the results for S -parameters of the developed tag with various values of L_f . It is noted that the tag antenna resonates around 2.45 GHz and 5.8 GHz and the L_f parameter somewhat affects the operating frequencies. Fig. 7 illustrates the input impedance with respect to the values of L_f . It is noticed that when L_f increases from 4.5 to 7.5 mm, the input resistance increases from 48.9 to 18.1 Ohm, and the reactance improves from 233.7 to 116.3 Ohm. But at the second operating frequency, the input resistance is around 28 Ohm, and the reactance is kipping around 47 Ohm. The optimized value of L_f is found to be 6.5 mm corresponding to $Z_{in} = (28.1 + j113) \Omega$ at 2.45 GHz and $Z_{in} = (27 + j40.3) \Omega$ at 5.8 GHz. These values are conjugate to the chip impedance Z_{chip} .

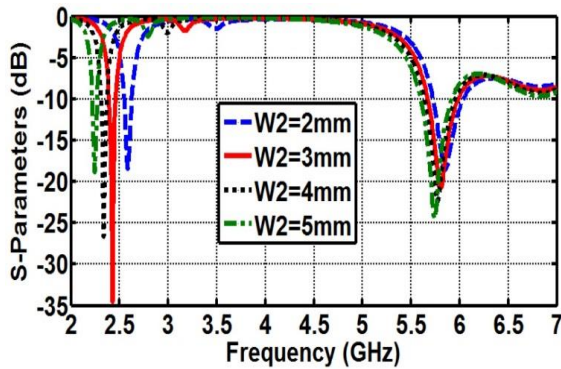


Fig. 4 – S -parameters for several values of W_2

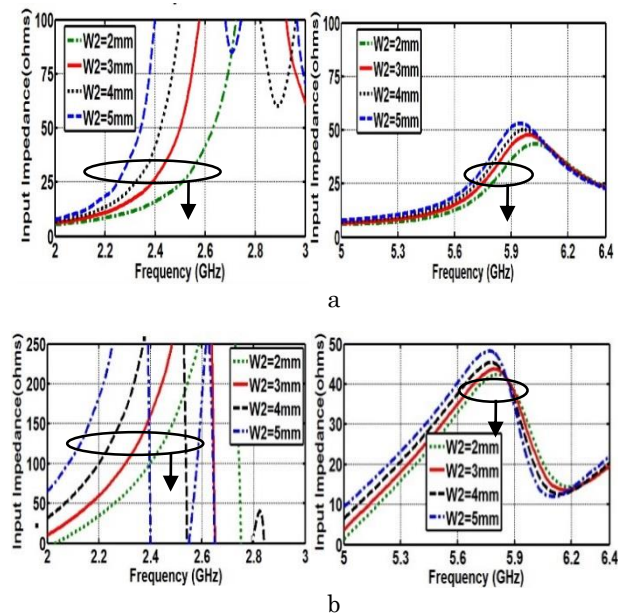


Fig. 5 – Results of the input impedance for different values of W_2 : real part (a), imaginary part (b)

3.3 Gain Study

The aim of this section is to examine the influence of different materials on the gain of the designed schematic diagram tag antenna. Fig. 8 shows the 3D model of the tag on several objects such as a human arm, a solution bag, and a bandage. The obtained results are presented in Fig. 9. The tag antenna only has a suitable gain, and the peak gain of the tag antenna shifts

from 2 to 3 dBi in the operational bands. Due to conductivity, high dielectric constant, and loss nature of objects, the gain of the tag antenna decreases in the first band.

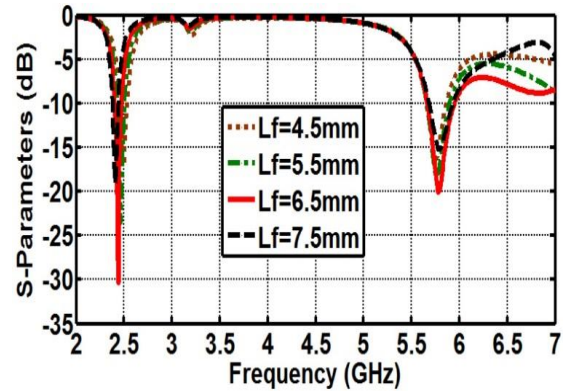


Fig. 6 – S -parameters for several values of L_f

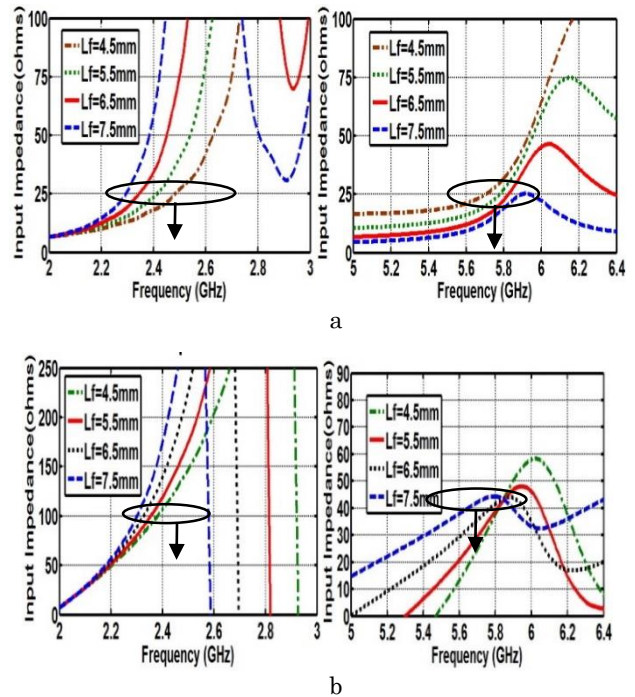


Fig. 7 – Results of the input impedance for different values of L_f : real impedance part (a), imaginary impedance part (b)

4. RESULTS AND DISCUSSION

4.1 Bands of Operation

Fig. 10 shows the S -parameters and input impedance of the intended tag. Significant reflection coefficients of -35 dB and -22 dB are observed at the center frequencies of 2.45 GHz and 5.8 GHz, respectively. The obtained -10 dB bandwidth (2.3-2.5 GHz and 5.78-6 GHz) covers the standards of Europe and India. At the operating frequencies, the tag antenna's input impedance values are changed close to the chip's complex conjugate impedance. The input impedances are $(28 + j114) \Omega$ and $(27 + j42) \Omega$ at resonate frequencies. The tag antenna's input impedance values are changed to almost equal the chip's complex conjugate impedance.

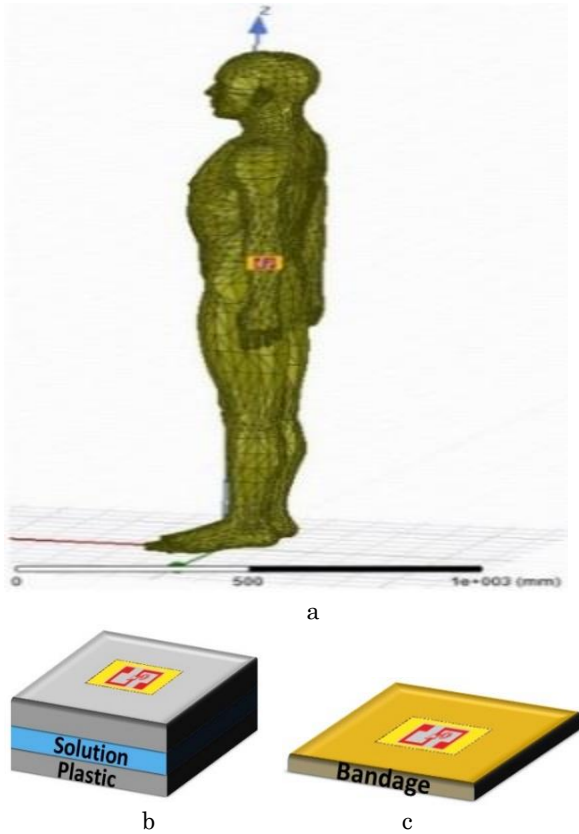


Fig. 8 – Simulation models of the recommended tag antenna: (a) human body, (b) solution bag, (c) bandage

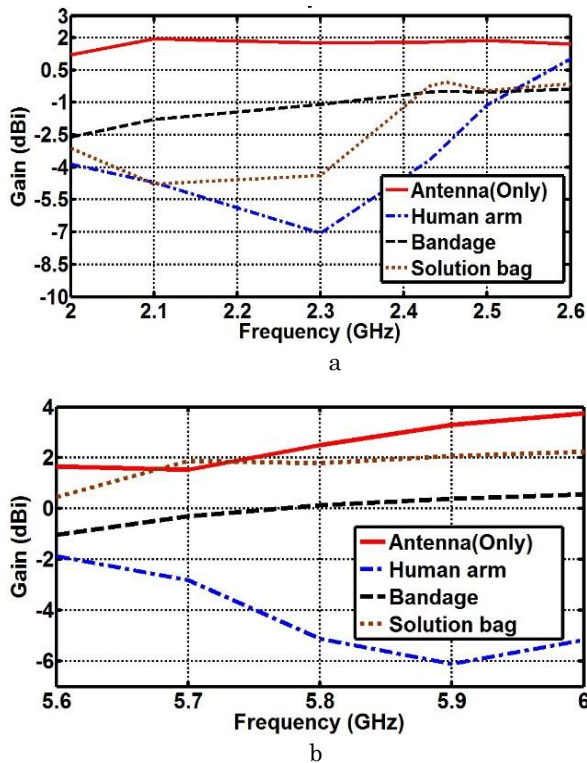


Fig. 9 – Simulated gain of the tag antenna on different materials: around the first band (a), around the second band (b)

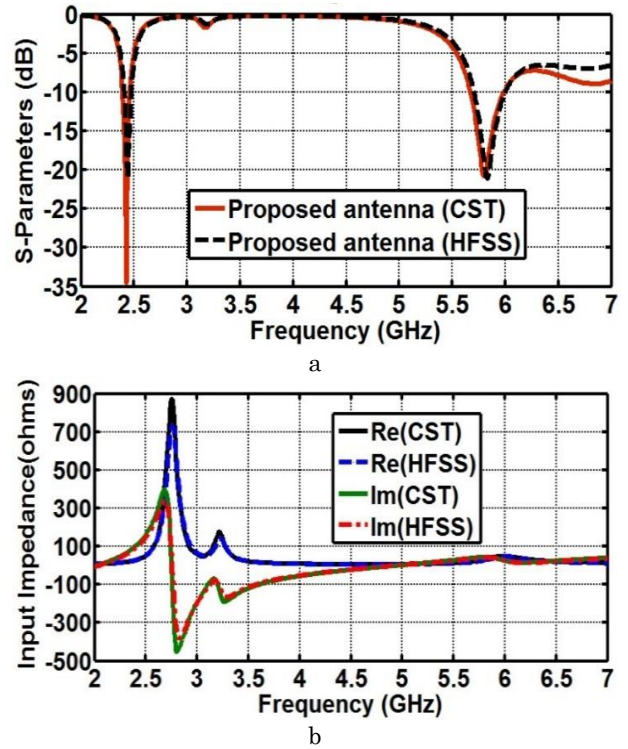


Fig. 10 – S-parameters (a), input impedance (b)

4.2 Current Distributions

We investigate the antenna component responsible for each operating frequency. As shown in Fig. 11, the surface current variations have been extracted.

The current is significantly focused on the meander line at 2.45 GHz with a minimum density on the rest of the tag surface. As a result, the meander line is important for producing the first frequency of 2.45 GHz. The surface current density is significantly concentrated at 5.8 GHz in the unit cell which is connected to the meander line. Hence, the tag antenna achieved the second operating frequency due to SRR.

4.3 Radiation Patterns

The finite integration approach is used to model the tag's 3D radiation pattern, which is shown in Fig. 12. The tag has maximum gains of 2.14 dBi and 3.22 dBi at the resonant frequencies of 2.45 GHz and 5.8 GHz, respectively.

5. CONCLUSIONS

In this work, an RFID tag has been investigated and proposed. The total physical size occupied by the antenna structure is 16×23×1.6 mm³. The tag results have been numerically validated using the finite element and integration methods. The recommended tag achieves two resonance frequencies around 2.45 GHz and 5.8 GHz. Furthermore, it provides better performance in terms of gain and radiation pattern. The performance has proven that the recommended tag is useable and can support multi-standard wireless remote healthcare applications.

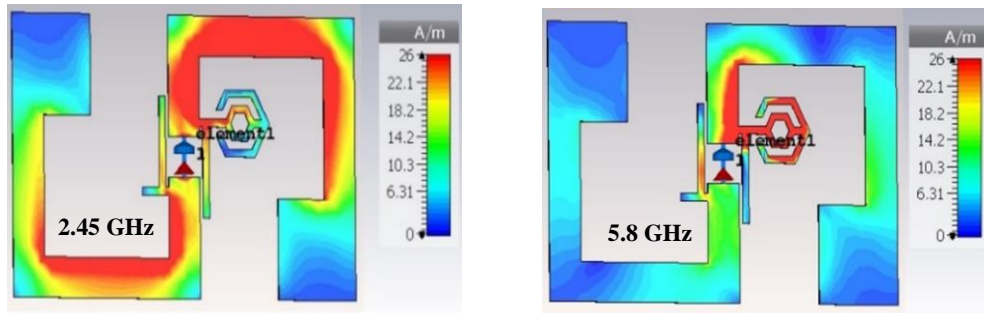


Fig. 11 – Current distribution of tag at resonant frequencies

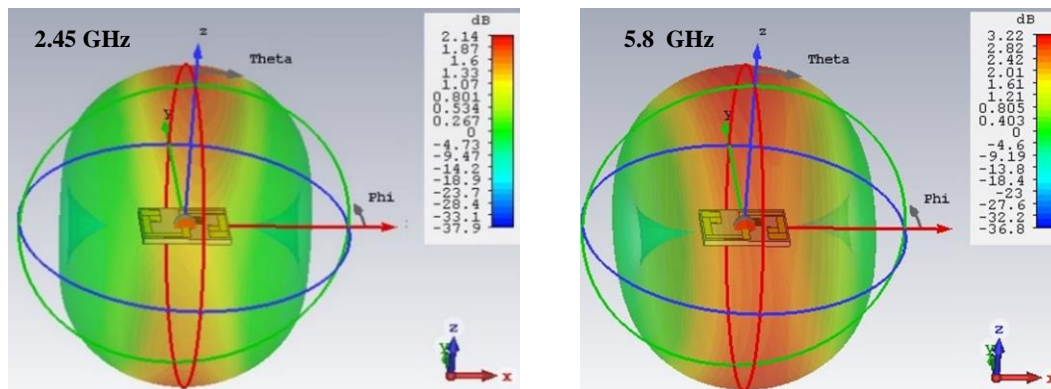


Fig. 12 – Gain of the recommended tag at several frequencies

REFERENCES

1. J.D. Hughes, C. Occhiuzzi, J. Batchelor, G. Marrocco *IEEE International Conference on RFID* (Atlanta, USA, 27-29 April 2021).
2. A.El Yassini, S. Ibnyaich, M.A. Jallal, S. Chabaa, A. Zeroual, *International Conference on Wireless Technologies, Embedded and Intelligent Systems (WITS)* (Fez, Morocco, 19-20 April 2017).
3. S. Bhaskar, A.K. Singh, *Int J RF Microw Comput Aided Eng*, **29** No 5, e21563 (2019)
4. A. El Yassini, M. Ali Jallal, S. Ibnyaich, A. Zeroual, S. Chabaa, *International Conference on Decision Aid Sciences and Application (DASA)* (Sakheer, Bahrain, 07-08 December 2021).
5. O. Saraereh, J. Jayasinghe, A. Andújar, J. Anguera, 2021 *International Symposium on Networks, Computers and Communications (ISNCC)*, (Dubai, United Arab Emirates, 31 October 2021 - 02 November 2021).
6. Byungje Lee, F.J. Harackiewicz, *IEEE Trans. Antenn. Propag.* **50** No 8, 1160 (2002).
7. A. El Yassini, M. Ali Jallal, S. Ibnyaich, A. Zeroual, S. Chabaa. *Instrumentation Mesure Métrologie*, **19** No 2, 83 (2020).
8. S.K. Sharma, R.K. Chaudhary, *IEEE Antenn. Wireless Propag. Lett.* **14**, 1670 (2015).
9. S. Ahdi Rezaeieh, M.A. Antoniadis, A.M. Abbosh, *IEEE Trans. Antenn. Propag.* **65** No 4, 2090 (2017).
10. A. C. Polycarpou, A. Dimitriou, A. Bletsas. P.C. Polycarpou, L. Papaloizou, *IEEE Antenn. Propag. Mag.* **54** No 4, 255 (2012).
11. S. Parlak, I. Marsic, A. Sarcevic, W.U. Bajwa, L.J. Waterhouse, R.S. Burd, *IEEE Trans. Mobile Comput.* **15** No 4, 924 (2016).
12. A. Sharif, J. Ouyang, K. Arshad, M.A. Imran, Q.H. Abbasi, *IEEE International Symposium on Antennas and Propagation and North American Radio Science Meeting* (Montreal, QC, Canada, 05-10 July 2020).

Компактна та мініатюрна дводіапазонна антена-мітка на основі метаматеріалу для IoT, технології RFID та додатків лікарняних послуг

Abdessalam El Yassini, Mohammed Ali Jallal, Saida Ibnyaich, Abdelouhab Zeroual

Physics Department, Faculty of Sciences Semlalia, Cadi Ayyad University, 40000 Marrakesh, Morocco

Дослідження пропонує компактну антenu-мітку для радіочастотної ідентифікації (RFID), яка забезпечує роботу в двох діапазонах: 2,3-2,5 ГГц і 5,78-6 ГГц. Структура антени-мітки складається з двох меандрових ліній, з'єднаних індуктивною петлею метаматеріалу. Топологія цієї конструкції пропонує такі переваги, як досягнення багатьох діапазонів, гарного узгодження імпедансу та діаграми спрямованості на резонансних частотах. Конструкція має невеликий розмір $16 \times 23 \times 1.6$ мм³. Запропонована антена-мітка виготовляється на підкладці FR4 з параметрами $\epsilon_r = 4,3$ і $\tan\delta = 0.022$. Антена-мітка має максимальний коефіцієнт підсилення 2,14 дБі та 3,22 дБі на резонансних частотах 2,45 ГГц та 5,8 ГГц відповідно. Представлено дослідження запропонованої мітки-антени з тілом людини, мішком для розчину та бинтом. Крім того, запропонована антена-мітка має гарні характеристики і підтримує два діапазони роботи, що підтверджує її придатність для технології RFID і дистанційних програм охорони здоров'я.

Ключові слова: RFID-мітка, IoT, Метаматеріал, Дводіапазонний режим, Додатки лікарняних послуг.